Description of a Glauconitic channel by AVO analysis

Yong Xu and John C. Bancroft

ABSTRACT

AVO analysis is performed on vertical component seismic data from a line in Blackfoot. *P* wave reflectivity (R_P) and *S* wave reflectivity (R_S) are extracted from the CDP gathers of vertical component data after true amplitude processing. A fluid factor section is obtained from R_P and R_S sections using the mud-rock line derived from local dipole sonic logs. By combining R_P and R_S sections and well logs, the Glauconitic channel can be better interpreted. On the fluid factor section, the Glauconitic channel exhibits a stronger and more detailed anomaly.

INTRODUCTION

AVO phenomena in the seismic data obtained, from a 1995 Blackfoot 3C-2D line have been investigated at CREWES since the line was acquired. The authors have applied Lame's parameter extractions from vertical component (Xu and Bancroft, 1998). The extracted Lame's parameters provide information to delimitate the Glauconitic channel zone. AVO modeling, parameter sensitivity analysis, and noise effect have been studied with this data set. Recently, R_P - R_S extraction and fluid factor calculation were computed. The subsequent results demonstrated a great improvement in the description of the Glauconitic channel.

METHOD

The fluid factor method was developed by Smith and Gidlow (1987) to locate anomalies that deviate from statistical relationship between V_P and V_S. Smith and Gidlow defined the fluid factor as

$$\Delta F = \frac{\Delta V_P}{V_P} - 1.16\frac{V_S}{V_P}\frac{\Delta V_S}{V_S} \quad . \tag{1}$$

Derivation of equation (1) uses Castagna's mud-rock line, which is a statistical relationship between V_P and V_S (Castagna, et. al., 1985) and defined as

$$V_P = 1.16V_S + 1360 \quad . \tag{2}$$

The $\frac{\Delta V_P}{V_P}$ and $\frac{\Delta V_S}{V_S}$ in equation (1) can be approximated by R_P and R_S in the usual cases, because density has much smaller relative change than V_P or V_S. The *P* wave normal incident reflectivity, R_P, and the *S* wave normal incident reflectivity, R_S, are extracted from CDP gathers following amplitude-preserved processing. The R_P and R_S extraction from seismic data is based on Aki-Richards' approximation for the *P-P*

reflection coefficient, $R_{PP}(\theta)$, which varies with incident angle, θ. Aki-Richards' approximation is reformatted as equation (3).

$$R_{PP}(\theta) = \frac{1}{2}(1+\tan^2\theta)\frac{\Delta Ip}{Ip} - 4(\frac{Vs}{Vp})^2\sin^2\theta\frac{\Delta Is}{Is} - [\frac{1}{2}\tan^2\theta - 2(\frac{Vs}{Vp})^2\sin^2\theta]\frac{\Delta\rho}{\rho} . \quad (3)$$

Equation (3) is approximated to equation (4) which shows sufficient accuracy in small incident angle ($< 40^o$) cases.

$$R_{PP}(\theta) = (1+\tan^2\theta)R_P - 8(\frac{Vs}{Vp})^2(\sin^2\theta)R_S . \quad (4)$$

In this study, the vertical component seismic data is carefully processed to preserve amplitude. The R_P and R_S sections are extracted from CDP gathers using equation (4). A mud-rock line is derived from local dipole sonic well logs. The fluid factor in equation (1) is modified using the new mud-rock line and fluid factor section is the obtained from R_P and R_S sections.

CASE STUDY—DESCRIPTION OF GLAUCONITIC CHANNEL

Figure 1 shows the location map of the 3C-2D seismic line 950278, the well controls and the incised valley isopach (Miller et. al., 1995). Two wells, 04-16 and 14-09, are used to form velocity models and to derive mud-rock line. The 04-16 well has dipole sonic logs, while well 14-09 does not have shear sonic log. Figure 2 shows a cross-plot of V_P and V_S of well 04-16 (the portion below 1000 m and above Mississippian formation). The fitted linear relationship and Castagna's mud-rock line are also plotted in this figure. The fitted line in equation (5), demonstrates different coefficients from Castagna's mud-rock line in equation (2),

$$V_P = 1.340V_S + 1150 . \quad (5)$$

From equation (5), a new fluid factor, with a slight difference from equation (1), is derived as

$$\Delta F = \frac{\Delta V_P}{V_P} - 1.34\frac{V_S}{V_P}\frac{\Delta V_S}{V_S} . \quad (6)$$

For comparison, the stack section of the vertical component data is plotted on Figure 3. The Glauconitic channel is located between CDP 140 and 165 at time of about 1050 ms. Mississippian formation (with weathered top) is below the channel. Figures 4 and 5 show the extracted R_P and R_S sections. The R_P section has better resolution than the stack section and the Mississippian top is clearer on the R_P section than on the stack section. The R_S section is noisier and less continuous than the R_P section. The Mississippian top is very weak on the R_S section, but the channel is clearer on the R_S section. In this study, the fluid factor section displays advantages over either the R_P or the R_S section. Figure 6 shows the fluid factor section, and

Figure 7 enlarges the time portion around the Glauconitic channel zone. In both figures, the Glauconitic channel anomaly is very strong and detailed.

CONCLUSIONS

Extracted R_P and R_S sections are informative to interpreted Glauconitic channel zone and lithology changes. The fluid factor section shows advantages in describing the Glauconitic channel. The derived mud-rock line helps to obtain fluid factor that is suitable to local geology.

ACKNOWLEDGEMENTS

The authors would like to thank the sponsors of CREWES project for their support.

REFERENCES

Castagna, J. P., Batzle, M. L., and Eastwood, R. L., 1985, Relationship between compressional wave and shear wave velocities in clastic silicate rocks: Geophysics, V50, 571 - 581.

Miller, S. L. M., Aydemir, E. O., and Margrave, G. F., 1995, Preliminary interpretation of P-P and P-S seismic data from the Blackfoot broadband survey: CREWES Research Report 1995, Chapter 42.

Smith, G. C., and Gidlow, P. M., 1987, Weighted stacking from rock property estimation and detection of gas: Geophys. Prosp. V35, 993-1014.

Xu, Y., and Bancroft, J. C., 1998, AVO case study: Extraction of Lame's parameters from vertical component seismic data: Geo-triad'98 abstracts, 350-351.

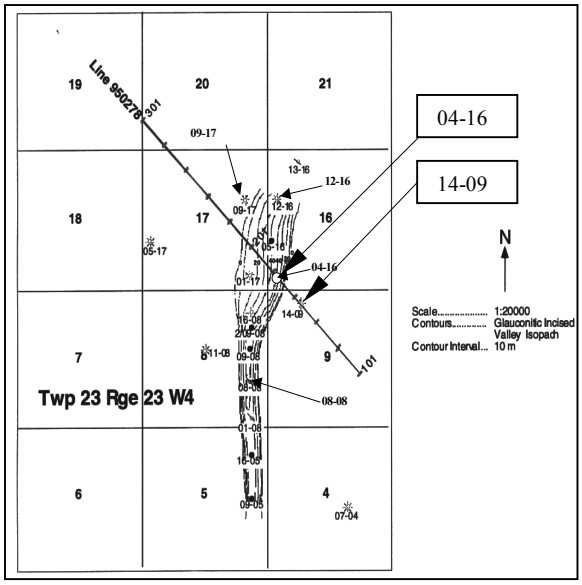

Figure 1. Location map of 3C-2D seismic line 950278, well control and the incised valley isopach (Miller et. al., 1995).

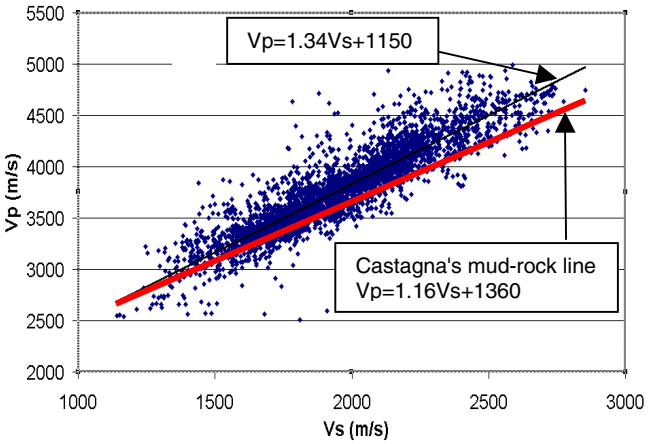

Figure 2. Cross-plot of V_P and V_S of well 04-16 (portion below 1000 m and above Mississippian formation).

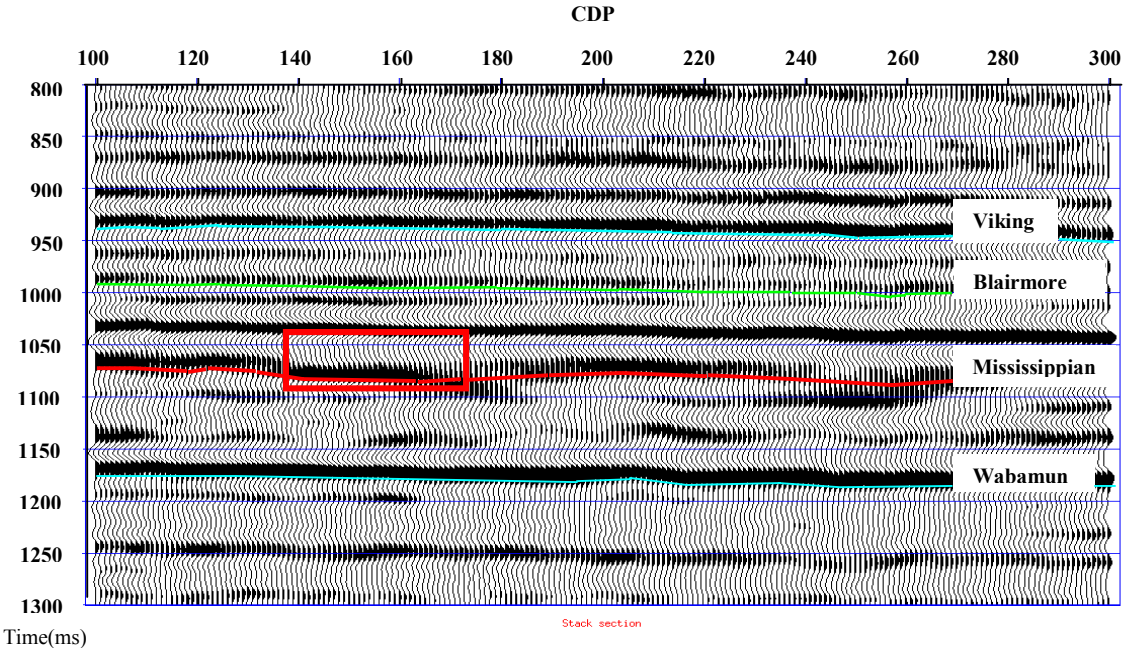

Figure 3. The stack section of vertical component seismic of 1995 3C-2D line. The NMO corrected CDP gathers, before AVO analysis, are stacked into this section. The box between CDP 140 and CDP 165, at around 1050ms shows the Glauconitic channel.

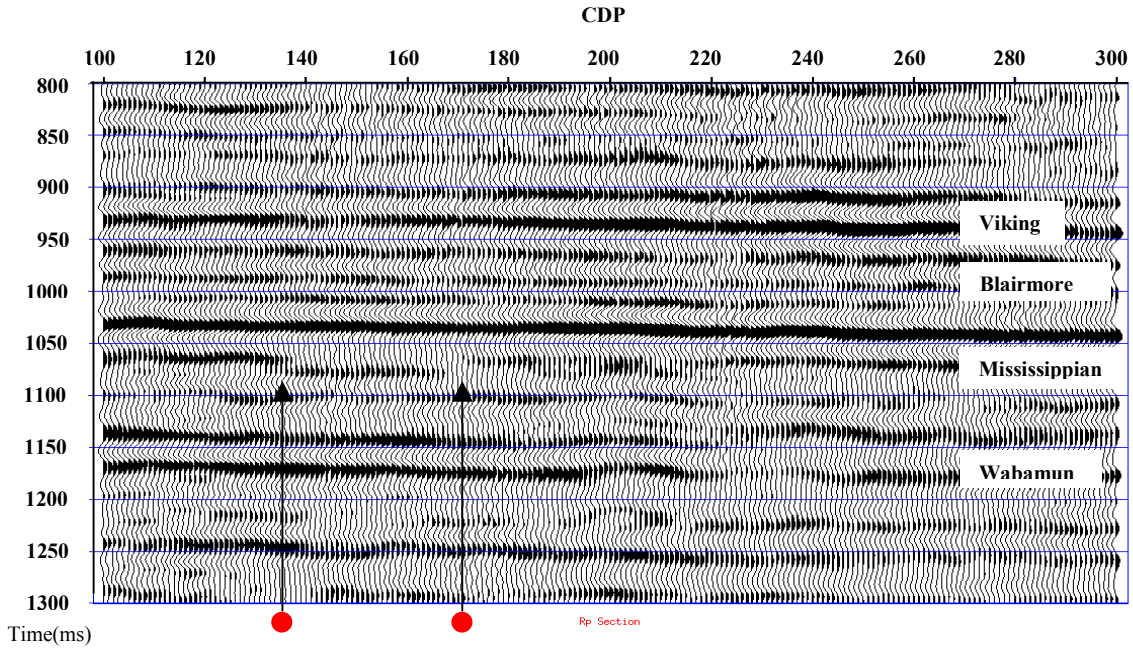

Figure 4. R_P section extracted from the CDP gathers of vertical component seismic data after true amplitude processing. The border of the Glauconitic channel is shown by two arrows. It is clearer than on Figure 3.

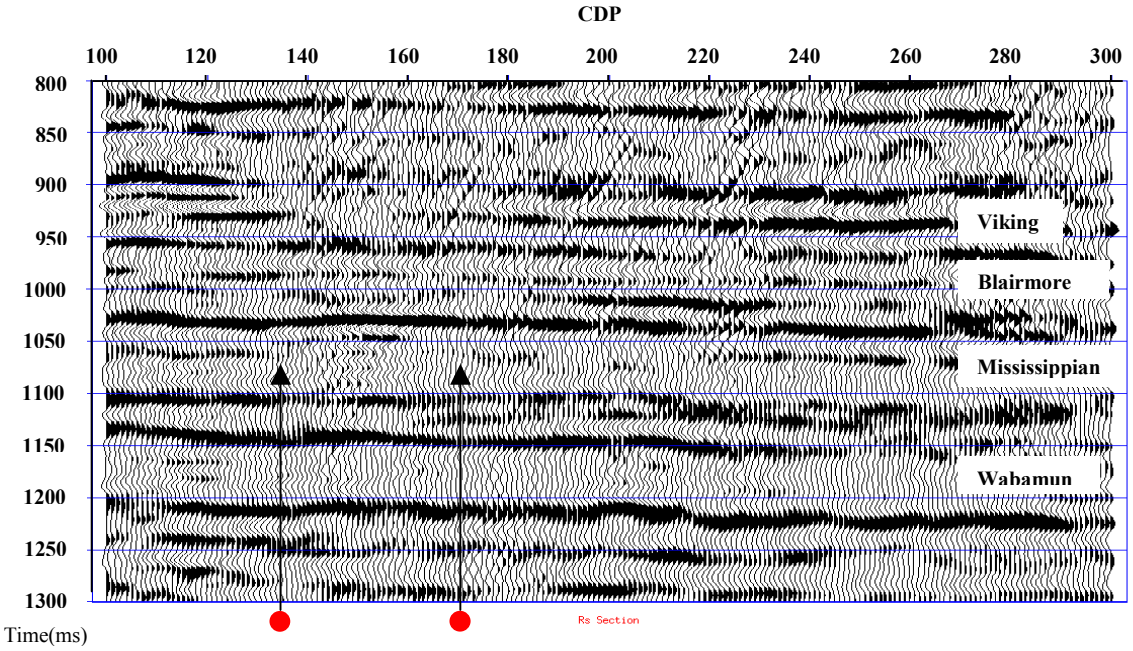

Figure 5. R_S section extracted from the CDP gathers of vertical component seismic data after true amplitude processing. The Mississippian top is weak between two arrows. But the Glauconitic channel on this section is more detailed than it is in Figures 3 and 4.

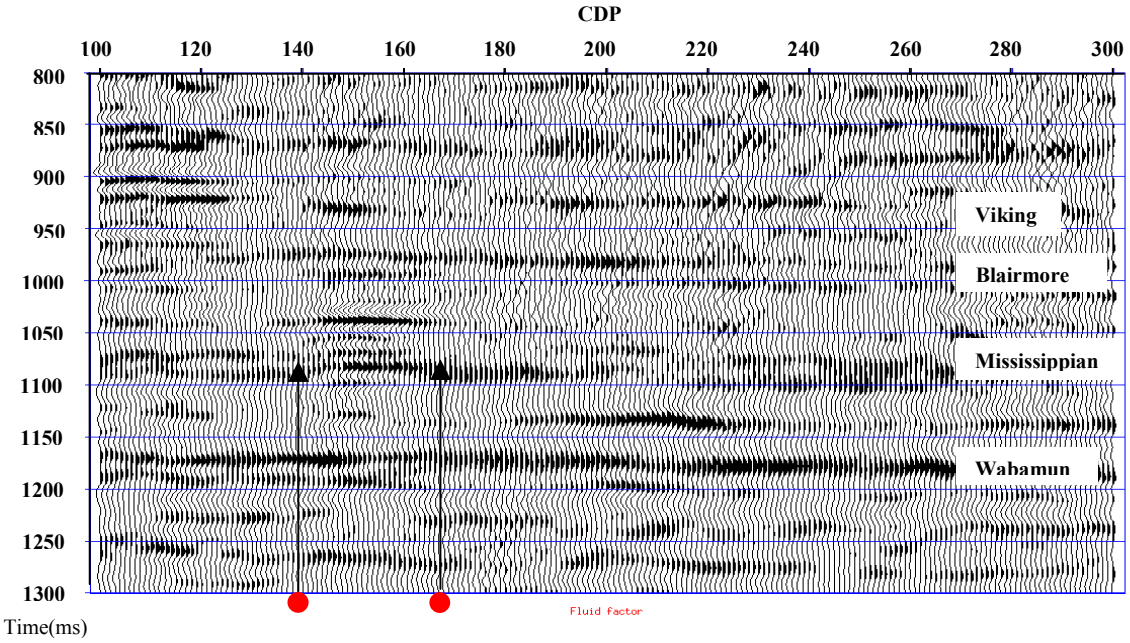

Figure 6. Fluid factor section obtained from R_P and R_S sections by applying equation (6). The Glauconitic channel is clearly seen as a strong and detailed anomaly between 1000ms and 1100ms at CDP 140 to CDP 165. The fluid factor exhibits a clear border and details of the Glauconitic channel.

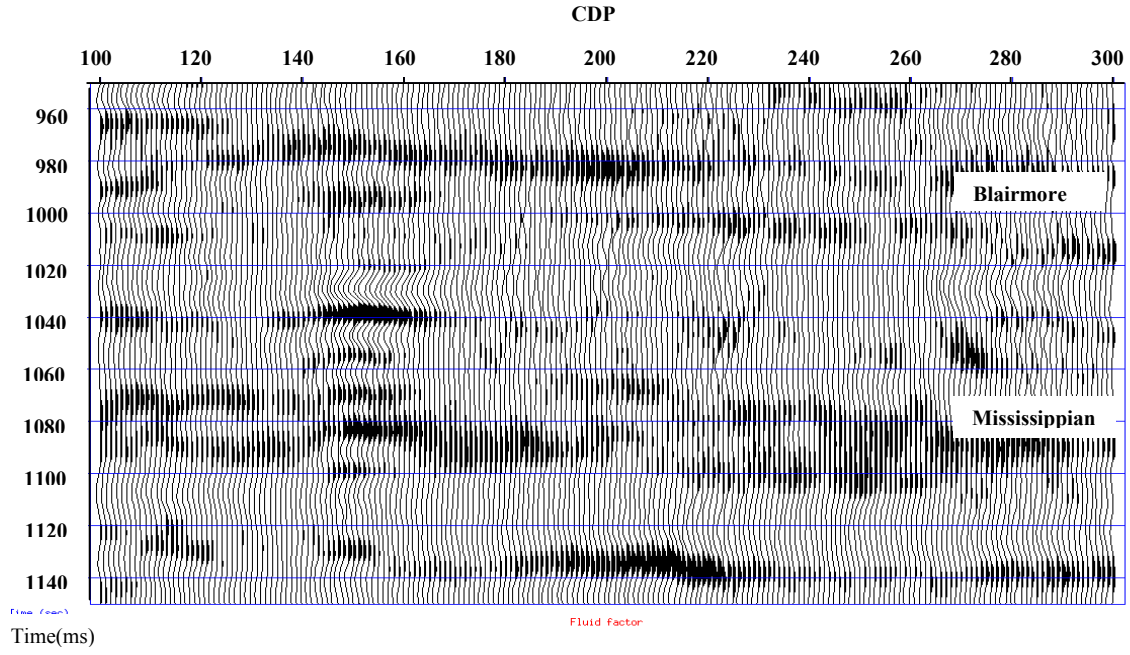

Figure 7. Enlargement of fluid factor section within the time portion between 950 ms and 1150 ms. The Glauconitic channel is distinguished between CDP 140 and CDP 165.